nature protocols

PROTOCOL EXTENSION

https://doi.org/10.1038/s41596-019-0230-y

Biomimetic smoking robot for in vitro inhalation exposure compatible with microfluidic organ chips

Kambez H. Benam[1,4,5], Richard Novak[1,5], Thomas C. Ferrante[1], Youngjae Choe[1] and Donald E. Ingber[1,2,3*]

Exposure of lung tissues to cigarette smoke is a major cause of human disease and death worldwide. Unfortunately, adequate model systems that can reliably recapitulate disease biogenesis in vitro, including exposure of the human lung airway to fresh whole cigarette smoke (WCS) under physiological breathing airflow, are lacking. This protocol extension builds upon, and can be used with, our earlier protocol for microfabrication of human organs-on-chips. Here, we describe the engineering, assembly and operation of a microfluidically coupled, multi-compartment platform that bidirectionally 'breathes' WCS through microchannels of a human lung small airway microfluidic culture device, mimicking how lung cells may experience smoke in vivo. Several WCS-exposure systems have been developed, but they introduce smoke directly from above the cell cultures, rather than tangentially as naturally occurs in the lung due to lateral airflow. We detail the development of an organ chip–compatible microrespirator and a smoke machine to simulate breathing behavior and smoking topography parameters such as puff time, inter-puff interval and puffs per cigarette. Detailed design files, assembly instructions and control software are provided. This novel platform can be fabricated and assembled in days and can be used repeatedly. Moderate to advanced engineering and programming skills are required to successfully implement this protocol. When coupled with the small airway chip, this protocol can enable prediction of patient-specific biological responses in a matched-comparative manner. We also demonstrate how to adapt the protocol to expose living ciliated airway epithelial cells to smoke generated by electronic cigarettes (e-cigarettes) on-chip.

This protocol is an extension to: *Nat. Protoc.* doi:10.1038/nprot.2013.137

Introduction

Development of the protocol

Evaluating the health impact of airborne compounds is critical to determining pathogenesis and mechanisms of injury. Cigarette smoking is the primary risk factor for the development of chronic obstructive pulmonary disease (COPD) and other lung disorders[1]. In addition, tobacco-related products, such as e-cigarettes are gaining popularity; however, the biological impact of their emissions on lung is poorly understood[2].

We recently reported how we leveraged human organ-on-a-chip (organ chip) microfluidic cell culture technology[3] to develop a breathing lung small airway-on-a-chip (small airway chip) lined with living human bronchiolar epithelium cultured at an air–liquid interface (ALI)[4] that also permits smoke exposure[2,5–10]. Although that work demonstrated the integration of physiologically accurate mechanical cues (i.e., fluidic shear and cyclic strain mimicking breathing in alveoli), we needed to develop both a small airway organ chip and a way of inducing physiological shear and dosing with smoke and other aerosols in the airway compartment to enable investigations of airway pathologies beyond the alveolus. This work builds on our earlier protocol used to develop microfluidic organ chips by incorporating a polyester track-etched membrane in combination with larger cross-section fluidic channels and a more streamlined fabrication process[11]. Although the preparation of small

[1]Wyss Institute for Biologically Inspired Engineering, Harvard University, Boston, MA, USA. [2]Harvard John A. Paulson School of Engineering and Applied Sciences, Cambridge, MA, USA. [3]Vascular Biology Program and Department of Surgery, Boston Children's Hospital and Harvard Medical School, Boston, MA, USA. [4]Present address: Division of Pulmonary Sciences and Critical Care Medicine, Departments of Medicine and Bioengineering, University of Colorado, Anschutz Medical Campus, Aurora, CO, USA. [5]These authors contributed equally: Kambez H. Benam, Richard Novak.
*e-mail: don.ingber@wyss.harvard.edu

Fig. 1 | Components of the BSR. a, Schematic of the biologically integrated method for analyzing effects of inhaled WCS using the engineered breathing–smoking apparatus in the microfluidic human lung small airway chip. Cigarettes are loaded onto a revolving wheel in a smoke generator (top left) that breathes freshly produced whole smoke directly in and out of the lumen of the upper airway channel of the human lung small airway chip microdevice (bottom left) using a microrespirator (bottom right). User-controlled programming software (top right) regulates various parameters of the breathing behavior (e.g., rate, pattern and duration of respiration cycle) and smoking topography parameters (e.g., puff time, smoke-in time, inter-puff intervals, puffs per cigarette, number of cigarettes per smoking session) to execute desired exposure. **b**–**d**, Photographs of the experimental setup. The smoke generator (right) and the microrespirator (left) within a biosafety cabinet (**b**) before placement into a tissue culture incubator (**c**). **d**, The tissue culture incubator is situated within a custom-designed acrylic cage, which is connected to the outside exhaust lines of the building. Scale bars, ~20 cm. **a**,**b**,**d** reproduced with permission from ref. [2], Elsevier.

airway chips is detailed in the protocol by Benam et al.[12], here we connected the small airway chip microfluidically to a biomimetic smoking robot (BSR). This combination of respiration driven by a smoking robot—which inhales and exhales whole smoke from burning cigarettes in and out of the epithelium-lined microchannel under dynamic conditions—recapitulated human smoking behavior[2] (Fig. 1). Using this platform, we were able to compare the effects of inhaled smoke on chips lined with living mucociliated airway epithelium isolated from healthy and diseased COPD patients and to study the effects of e-cigarettes on human lung molecular-, genetic-, cellular- and tissue-level responses in vitro[2]. This protocol provides additional technical details to assist researchers in replicating small airway chip studies of smoke impact under physiologically and clinically relevant conditions; we hope our protocol will stimulate further applications for use with other organ chips, in vitro cultures and in vivo animal studies of smoke and aerosols.

The BSR recapitulates the mechanics and dynamic inhalation behavior of a smoker to facilitate study of smoking styles or topographies under realistic conditions with dynamic smoke generation. The system consists of three components: (i) a smoke generator, (ii) a microrespirator and (iii) LabVIEW control software that couples the two hardware components to create programmable smoking behavior. The compact smoke generator holds up to ten cigarettes or e-cigarettes inside a revolving holder. Custom silicone gaskets are designed to provide airtight seals around each cigarette and mechanical support while still allowing for ease of removal and cleanup. The revolver slides against a spring-loaded Teflon mouthpiece that forms a rotary seal and connects the cigarette being burned to a downstream vacuum pump protected from tar deposition by a disposable filter. Following ignition, the pump turns on using a fully automated resistive heating coil, which was selected to minimize environmental heating when placed inside a tissue culture incubator. The pump airflow is calibrated to be similar to that experienced by an adult human during inhalation, and it is synchronized with the microrespirator action so that each puff of smoke from a cigarette is generated only during an inhalation step, thus facilitating dynamic smoke generation and exposure. A smoke reservoir is used to provide a small buffer volume (5 ml) to decouple scaling up of the microrespirator volumes without affecting airflow through the cigarette. The entire smoke generator is positioned inside a smoke containment case with an active exhaust to a chemical vent to minimize exposure of smoke to the researcher and laboratory. By developing a compact design that can fit inside a standard tissue culture incubator, the tubing distances are reduced and maintained at the same temperature and humidity as the cell cultures, which minimizes loss of smoke components due to adsorption and condensation.

The microrespirator consists of eight glass gas-tight syringes actuated in parallel by two synchronous stepper motors and screws, with each syringe dedicated to a single exposure chamber. The syringe volumes and their displacements can be adjusted to meet the demands of both microscale organ chips and macroscale exposure chambers (e.g., for studies with standard culture plates or animals). As the microrespirator cycles through arbitrarily defined inhalation–exhalation steps, a valve in the smoke generator switches between air in and air out to waste, while a second valve switches the air input between fresh air samples from just outside the smoke generator and the dynamically generated smoke source. Thus, the exposure chamber is continually under bidirectional air flow, which permits programmable dynamic smoke exposure, as well as physiologically accurate non-smoking control conditions.

The LabVIEW control software and interface not only link the two hardware components, they also enable programming of an arbitrary smoke topography. Ignition times, inhalation times, puff duration, inter-puff intervals and other parameters can be incorporated into the program to model the smoking typography of real-world smokers. The interface and hardware also leave room for the automation of other components, such as additional valves or switches, which can be used to expand the current capability.

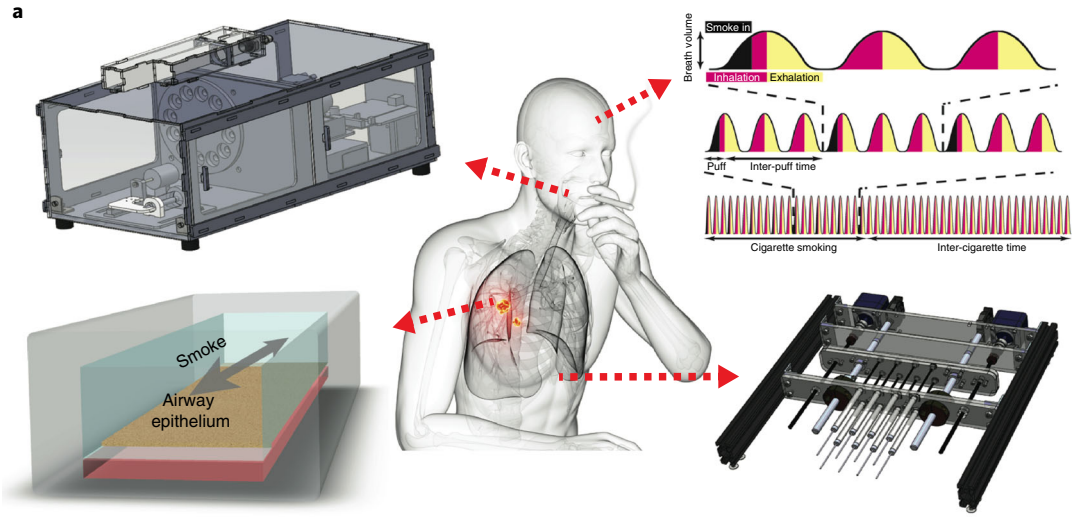
a
Smoke in
Breath volume
Inhalation
Exhalation
Puff
Inter-puff time
Cigarette smoking
Inter-cigarette time
Smoke
Airway
epithelium

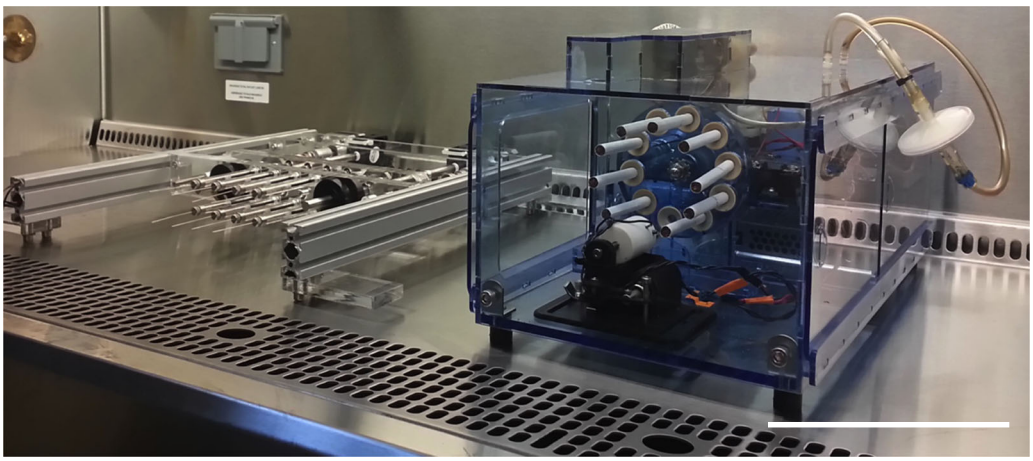
b

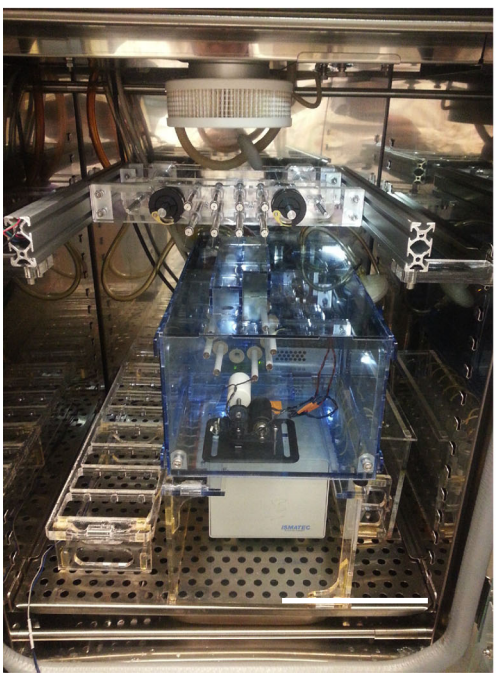
c


d

The BSR represents a compact and low-cost tool for testing various tobacco and tobacco-free cigarette products in a manner that mimics in vivo smoke exposure. By placing both the smoke generator and microrespirator inside a tissue culture incubator, it is possible to replicate in vivo smoking conditions more accurately. Temperature and humidity can be maintained to avoid smoke condensation in air lines or drying of exposed tissue. Furthermore, the distance between the source of the smoke, the air actuator and the central exposure chamber can be scaled to mimic the distance between the mouth and diaphragm, with appropriate scaling of air flows and tubing diameters. Through this biomimetic design approach, it is possible to alleviate many of the difficulties present in other systems, which often necessitate extensive empirical calibration for a specific experimental setup and smoking topography.

Applications

The BSR is a versatile and compact system that could be applied to any airtight exposure chamber, including animal cages, conventional cell culture plates and Transwell insert cultures with cells grown at an ALI, as well as to microfluidic organ chips. The exposure chamber is placed between the smoke source ('mouth') and the microrespirator ('diaphragm/rib cage') to mimic the bidirectional breathing motion experienced in the human lung. Using this approach, it is possible to generate a puff of concentrated smoke during the onset of inhalation (typically 30–50 ml in an average adult smoker), followed by clean air for the remainder of the ~500-ml inhalation. This pulse–chase action faithfully replicates clinically observed human smoking behavior and avoids the need for empirical dilution of smoke as is commonly performed for continuous smoke exposure systems. The dynamic smoke generation capability of the BSR enables replication of arbitrary human smoking behaviors for in vitro studies, and it could be used to enhance animal exposure studies as well.

For our studies, the BSR system was used to assess response of human small airway chips to breathing of fresh air or to an intensive nine-cigarette smoking regimen using chips lined by airway epithelial cells from three different healthy non-smoking donors and three donors with COPD[2]. In this acute model of smoking, the cells on the small airway chips remained alive and recapitulated the in vivo response to smoke exposure at multiple levels of analysis. Microparticles from the smoke were observed to be evenly distributed throughout the exposure region of each organ chip. Analysis of gene expression profiles revealed an induction of an oxidative stress response similar to that seen in human subjects; hemoxygenase 1 and various cytokines were upregulated, and ciliary beat frequency (CBF) was decreased as well. Furthermore, the BSR allowed for matched comparative analysis of responses of tissues from the same non-smokers to fresh air breathing or smoking conditions simultaneously, which is impossible in clinical studies. This unique and valuable feature reduced the variability of responses because it enabled strictly differential measurements, which take into account individual genetic variation as opposed to traditional comparisons of subject averages. Using the BSR, we identified novel biomarkers for COPD-specific responses to smoke, opening up avenues for therapeutic discovery.

Similar to commercially available cigarette smoke-generating machines, such as Baumgartner–Jaeger, Teague TE-10 and Vitrocell VC 10 systems (refs. [13–18]), we speculate that BSR can be applied to non-microfluidic in vitro cell culture systems (e.g., Transwell inserts) and animal exposure studies. For in vitro experimentation using commercial smoking machines, the exposure system is composed of a cell culture–containing sealed chamber that has two ventilation holes: one for the whole smoke to enter and the other (subjected to vacuum-driven negative pressure) for the exhaust to leave[15]. As such, utilizing the same exposure chambers[15,18], we contemplate that the existing smoke machines and their associated exhaust-removal systems can be replaced with the BSR. Similarly, animal inhalation cages—instead of being connected to off-the-shelf smoke generators[13,14]—can hypothetically be connected with the BSR. The advantage of using BSR in both in vitro and in vivo cases can be summarized by its small size and ability to deliver small volumes, which provides a greater range for end users to test various doses of fresh whole smoke.

The BSR is a versatile, dynamic exposure system with applications beyond tobacco smoking. Non-tobacco products are expanding, but regulation and understanding of health impact have lagged. Aerosol exposure in the context of environmental contaminants, workplace hazards, chemical and bioweapons, and other sources could be readily analyzed by the addition of an aerosol source or air sample through the mouthpiece. The compact and modular format, coupled with ease of scaling air volumes, makes the BSR a versatile instrument for airborne agent studies.

Alternative methods

Several experimental methods have been developed to assess the effects of inhaled aerosols generated by conventional and e-cigarettes on living cells in vitro[2,15,19–21]. Overall, these model systems can be divided into two types: one that generates and applies 'smoke fractions' and another that enables analysis of 'whole smoke'. The former is less challenging, but it contains only certain components of whole smoke, namely cigarette smoke extract (CSE) or cigarette smoke condensate (CSC)[22–25], and the latter is a more complex method that permits biological analysis of freshly generated smoke aerosols[15,19–21].

CSE has been most widely used in past studies[22,23,26–28]. It is generated by passing whole smoke through a liquid, generally cell culture medium, which leads to capture of only hydrophilic components from both particulate matter (PM) and the volatile phase of the smoke[29]. Thus, it lacks the hydrophobic fraction of whole smoke, and there is also uncertainty as to exactly which smoke chemicals are contained within CSE. In addition, the bioavailability of captured volatile molecules is not well characterized and, as such, CSE must be freshly prepared just before exposure to cell cultures. CSC is generated by capturing only PM of WCS on a filter[29], which normally constitutes <5% of all smoke constituents[20], and not the gas phase. It does not necessarily need to be freshly created, and the PM at the time of exposure is eluted in a solvent, such as dimethyl sulfoxide, which is subsequently diluted in cell culture medium[29]. Although CSE- and CSC-treated lung epithelial cell cultures can mimic certain biological phenotypes associated with smoke exposure, such as induction of cellular stress[25,26,30], addition of these materials disrupts the physiological ALI of the airway epithelium; this method also presents only fractions of whole smoke and fails to reproduce smoking topography (i.e., the complex dynamic patterns of smoke inhalation and expiration and other smoking-related behaviors), which has been demonstrated to substantially impact nicotine dose and carcinogen exposure[31,32].

Several whole-smoke exposure systems have been developed to address the challenges associated with CSE and CSC; these include the Baumgartner–Jaeger, Teague TE-10 and Vitrocell VC 10 systems[13–21] that we briefly mentioned above. These platforms offer three major advantages over CSE and CSC methods: (i) they support full interactions between the PM and the gaseous phase of the mainstream smoke, (ii) cells are exposed to the whole smoke without disrupting the ALI and (iii) they can mimic a number of smoking topography parameters. However, they are unable to reproduce physiological breathing air movements, which are responsible for delivering smoke to the lung airway lining. Specifically, they introduce WCS directly from above the cell cultures, rather than tangentially as naturally occurs in the lung due to lateral airflow and resulting shear forces associated with WCS exposure in human smokers. Because the systems do not integrate bidirectional airflow control with smoke generation, they require empirical smoke dilution, resulting in homogeneous smoke concentrations during exposure as opposed to the dynamic smoke dilution observed in human smokers[33]. In addition, due to the large size of the equipment (e.g., Baumgartner–Jaeger, Teague TE-10 and Vitrocell VC 10 systems), significant effort is required to calibrate smoke dosing to account for loss due to adsorption and condensation of smoke components in connecting tubing over relatively long distances at non-physiological temperatures. Compared with the Vitrocell VC 10 (refs. [16,18]), a representative commercially available smoking machine, our platform offers these major advantages: (i) it simulates active (not passive or sedimentary) smoke exposure under rhythmic breathing airflow movements to execute smoking topography; (ii) it features a shorter tubing distance for smoke to travel to reach the living tissue, thus resulting in potentially less smoke particulate loss, because the whole apparatus fits into a cell culture incubator; (iii) it has microfluidic compatibility to connect with organs-on-chips; and (iv) it occupies much less space. Nevertheless, some benefits of using systems such as the Vitrocell VC 10 include ability to program the smoking process, ease of cleaning the instrument and flexibility to incorporate additional analytical tools, for instance, those required for quantification of total particulate matter from fresh WCS.

Limitations

The current design of the smoke generator accepts only up to ten cigarettes or other tobacco and non-tobacco products. The revolver could be expanded to hold more, and a cigarette loader or hopper could also be integrated for an even greater capacity and to extend the time between refilling. Another limitation is the current incompatibility of using cigarettes and e-cigarettes simultaneously due to the need for external ignition for traditional cigarettes, which can damage e-cigarettes. However, this could be programmed into the software to tie specific automation steps to unique mouthpiece locations.

The current design has a fixed pump air flow rate setting controlled by an on/off switch. This has been calibrated to handle the replaceable air filter that is used to avoid pump damage due to tar buildup. As a result, the smoke generator pump does not burn the cigarette with exactly the same airflow profile as the microrespirator. This limitation could be addressed by replacing the on/off pump control with voltage control. The voltage could be calibrated to pump flow rate, enabling modulation of the cigarette burn rate in addition to control of the smoke delivery profile.

The smoke generator enclosure is designed to remove smoke from the experimental area, particularly during inter-puff intervals, when the cigarette smoke is directed into the large smoke chamber as opposed to being sucked into the reservoir and to waste. The secondhand smoke is therefore vented out to a chemical vent and not sampled. However, by modifying the hardware, it would be possible to redirect the smoke input tube from the small smoke reservoir to the chamber containing the burning cigarettes to sample secondhand smoke during a specific smoking topography program.

The BSR has been optimized specifically for use with small airway chip technology, and although it is potentially applicable to alternative biological model systems (e.g., animals and conventional cell culture plates), we have not yet adapted it for such applications, but this could be pursued in the future. Because this is a first-of-its-kind, microfluidically coupled, multi-compartment system that bidirectionally 'breathes' WCS through microchannels of an organ chip, certain characterizations, such as dosimetry, gas vapor and particulate-phase characterization, aerosol-size determination, and assessment of aerosol evolution, aging and losses in the system are lacking. Similarly, it will be necessary to more thoroughly characterize biological responses (e.g., induction of oxidative stress after smoke exposure) and correlate them with aerosol characterization data. All of these will need to be addressed in future studies.

Last, the microrespirator described here is limited in scaling of the breathing volume because of motor output and size constraints. Although the current design should be able to handle up to 80 ml in total volume per 'breath' (using eight 10-ml syringes), this could limit the size of the animal cage or other large exposure chamber that could be integrated into the present design. If a larger cage/chamber is desired, a larger pump, including a diaphragm pump similar to the one used for cigarette burning, could be used to provide bidirectional airflow with much larger volume capacity.

Overview of the protocol

The construction of the BSR system, consisting of the smoke generator assembly (SGA) (Steps 1–17), microrespirator assembly (Steps 18–24), incubator installation (Steps 25–31), software setup and parameter programming (Steps 32–39), must be carried out before it can be used to conduct a smoke exposure study. Here, we focus on use of the BSR in combination with human small airway chips, so we describe small airway chip fabrication (Step 40), culture (Steps 41–49) and subsequent execution of a smoke study (Steps 50–57), as well as methods for its termination (Steps 58–63). We have previously reported the detailed protocol for fabricating the small airway chips, culturing primary lung airway epithelial cells under an ALI and guiding their differentiation into mucociliated epithelium on-chip[12], so we include only a brief summary of those steps. We also explain how to clean the BSR following an inhalation exposure study. In addition, we include several optional protocols for organ chip analysis: qRT–PCR (Step 64A), whole-genome microarray expression (Step 64B), western blot (Step 64C) and CBF (Step 64D) analyses following smoke challenge. We recommend that users include control chips for each study and treat them in a separate incubator using identical breathing actuation but using incubator air and not smoke. The use of bidirectional air shear for controls allows for examining the role of smoke exposure without confounding its means of delivery. The full workflow for running the experiment is provided in Fig. 3; Supplementary Video 1 shows an overview of the BSR and its implementation.

Experimental design

Gasket molding

Gaskets for cigarettes and e-cigarettes consist of two custom silicone parts manufactured by casting 3D-printed molds (design files provided in the Supplementary Information). Print gasket molds are made, using stereolithography, from Prototherm 12120, Acura 60 or a similar polymer with smooth untextured surfaces and a heat deflection temperature of at least 60 °C. This task can be outsourced to various vendors (e.g., Protolabs) or performed in-house if 3D stereolithography printing equipment is available.

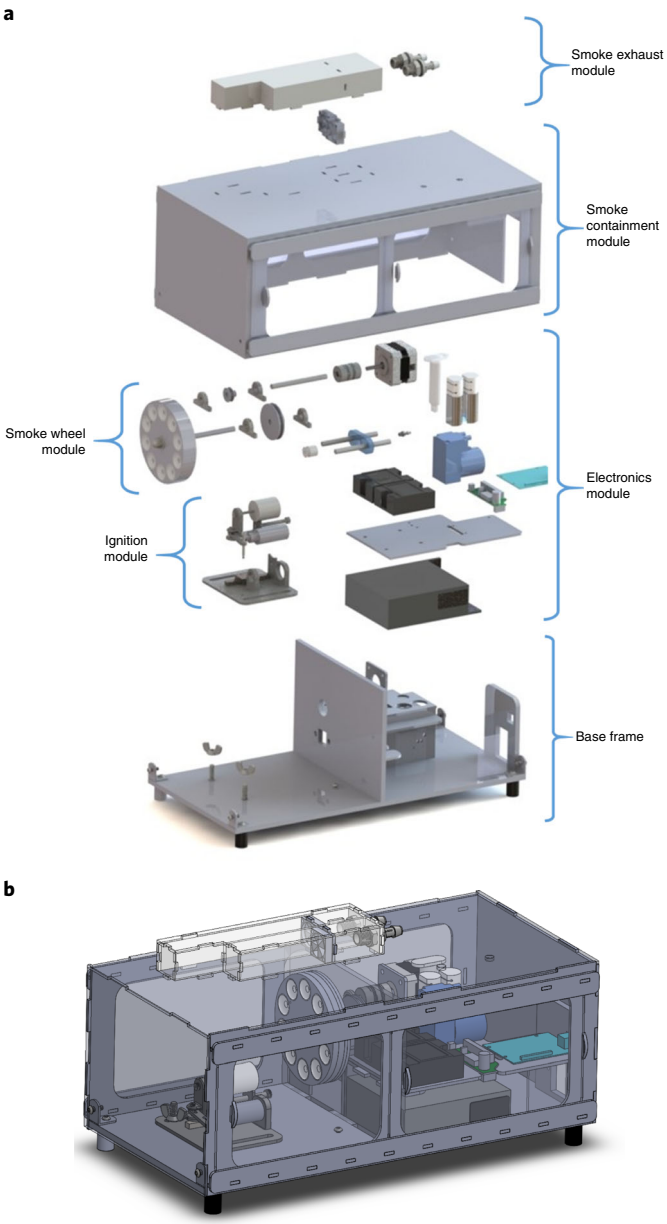

Fig. 2 | Overview of the smoke-generating system. a,**b**, Illustration of smoke generator module, highlighting the subassemblies and components (**a**) and the compact assembled system with a smoke containment cover (**b**). The smoke generator module readily fits into a standard cell culture incubator.

Smoke generator construction

The smoke generator is designed to be constructed using prototyping tools available in most university shops and relies primarily on laser-cut and glued acrylic sheets to create mounts and supports for the mechanical, pneumatic and electrical components, as well as the smoke containment housing (Fig. 2 and Supplementary Figs. 1–5). Laser cutter settings are specified for an Epilog 75 W instrument, but these settings may need to be optimized for a different brand of power laser cutter. Users should assemble the separate hardware modules of the smoke generator shown in Fig. 2a according to the diagrammed instructions in Supplementary Figs. 1–5. This enables testing of each component's function and simplifies assembly of the complex instrument. Each module should be assembled separately using acrylic cement. The Teflon mouthpiece (Supplementary Fig. 3d) should be turned on a lathe to produce a concentric flexible gasket that can slide easily along the cigarette holder smoke wheel while providing an airtight seal. The lighter housing of the ignition assembly (Supplementary Fig. 4e) is machined from Teflon to provide a mount for the thermally insulating ceramic rod that

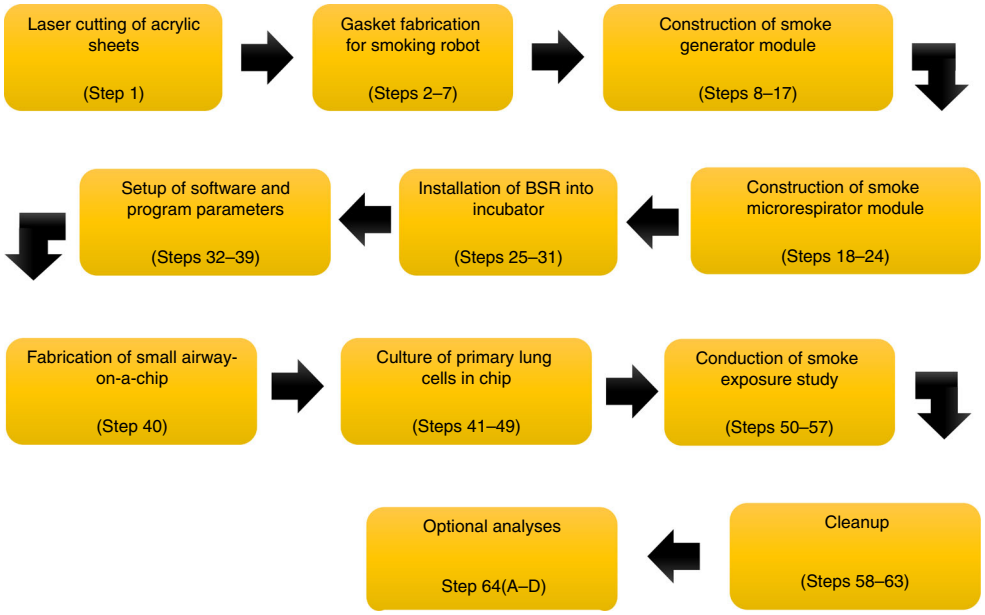

Fig. 3 | Schematic of workflow for assembly of a BSR and conduction of small airway chip smoke exposure studies. Step numbers correspond to the procedure steps in the text.

supports a NiChrome wire heating coil. The design enables assembly of hardware before integrating the electrical components and tubing. Figure 3 describes the workflow required to fabricate a BSR and implement it in smoke exposure studies with the small airway chip. Use of disposable tubing throughout the smoke pathway allows for easy decontamination between studies while enabling a bidirectional airflow pattern through the implementation of solenoid pinch valves (Fig. 4). This approach provides a low-cost strategy for construction and further prototyping that can be broadly applied in both academic and industrial research environments.

Microrespirator construction

The microrespirator is designed to be inserted as a shelf in a standard incubator to minimize use of valuable incubator space; however, it also could be hung on the incubator wall. The components are all standard parts readily available from most engineering supply companies, and an Arduino-based control system was developed to allow stand-alone use independent of the smoke generator for other laboratory applications and as a non-smoking, breathing-only control for organ chip smoke exposure studies. Assemble separate hardware components of the microrespirator according to the diagrammed instructions in Supplementary Fig. 6.

Incubator installation

A dedicated incubator with adequate smoke containment and ventilation should be used for all smoking studies to avoid exposure of researchers to smoke. The ventilation duct must accommodate exhaust tubing from the smoke generator module, which is used to vent secondhand smoke as well as exhaled firsthand smoke from the smoke generator and organ chips. A properly designed containment and exhaust system enables studies of other inhaled materials and reagents, such as smog, nanoparticles or chemical vapors, with minimal modification of the BSR. Follow proper incubator-handling protocols whenever installing or removing components from the incubator. The incubator should be routinely cleaned and decontaminated, and all materials entering the incubator should be disinfected with 70% ethanol or biocidal spray. Care should be taken to avoid use of solvents or corrosive reagents that could damage the acrylic or metal components of the BSR.

Software setup

The overarching control software consists of a LabVIEW interface that communicates with two Arduino microcontrollers (smoke generator and microrespirator) (Fig. 5). The software allows for smoking topography parameter programming, as well as modification of other settings, such as ignition time, ignition air intake volume and hardware communication. In addition, the control

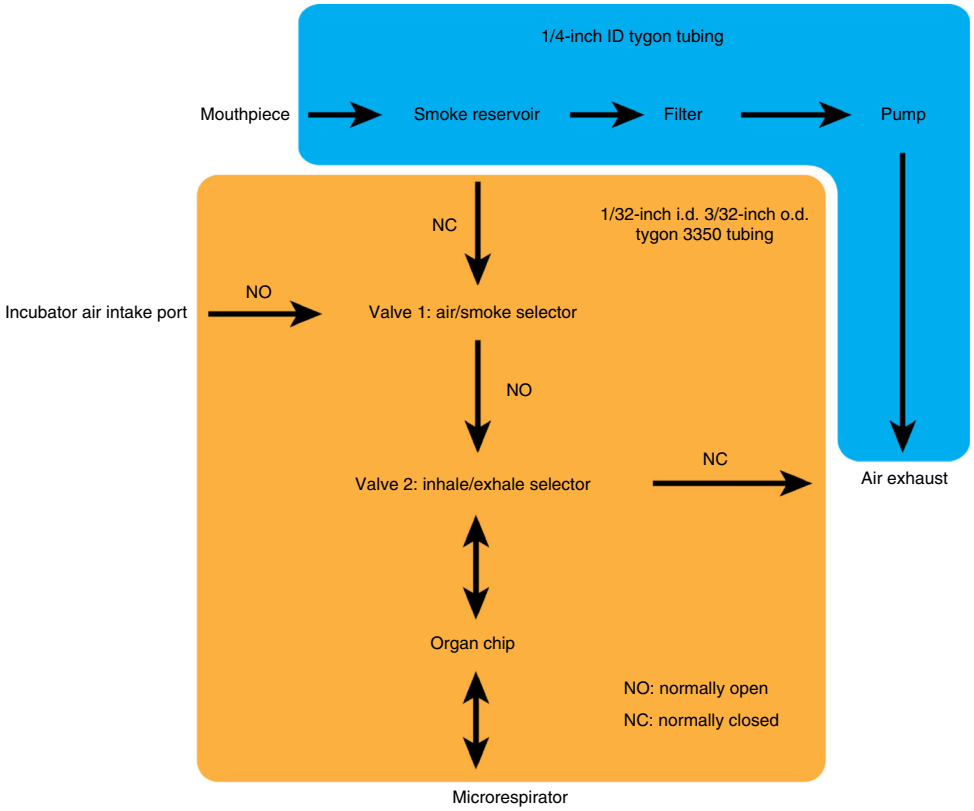

Fig. 4 | Schematic of the airflow in the BSR. The orange box highlights the parts of the system that mimic the human respiratory tract, whereas the blue region delineates the mouth and external environment. Each region uses the specific tubing indicated for connecting components, and arrows indicate airflow direction. Programmable valves switch between incubator air and smoke according to the programmed smoking topography. Organ chips connected to the microrespirator experience an in vivo–like bidirectional airflow pattern.

interface allows for switching between traditional cigarettes and e-cigarettes. The control toggles between motor actuation for multiple cigarettes and lack of motor actuation due to the large capacity of a single e-cigarette compared to a single traditional cigarette. Although the e-cigarettes are inserted into the BSR revolver just as traditional cigarettes are, mechanical support in the form of a support bar or cradle can avoid misalignment due to the higher mass of e-cigarettes.

Materials

Biological materials

- Human primary small airway epithelial cells (PromoCell, cat. no. C-12642; Lonza, cat. no. CC- 2547) ▲ **CRITICAL** The cells used should be regularly checked to ensure that they are not infected with mycoplasma.

Reagents

- Small airway epithelial cell basal medium (PromoCell, cat. no. C-21270) and small airway epithelial cell growth medium supplement pack (PromoCell, cat. no. C-39170) ▲ **CRITICAL** This culture medium and supplement pack are optimized for growth of small airway epithelial cells in the chip.
- DMEM-high glucose with L-glutamine, phenol red and sodium pyruvate (Thermo Fisher Scientific, cat. no. 11995065) ▲ **CRITICAL** DMEM-high glucose is required when differentiating small airway epithelial cells into mucociliated cells at the ALI on-chip.
- Collagen I (rat tail; Corning, cat. no. 354236) ▲ **CRITICAL** It is important to coat the porous membrane in chips with collagen before cell seeding.
- Research-grade 3R4F cigarettes (obtainable from Kentucky Tobacco Research & Development Center, College of Agriculture, Food and Environment, University of Kentucky) ▲ **CRITICAL** These reference cigarettes have defined constituents, such as tar, nicotine and various blends, and enable more accurate comparison between studies.

a

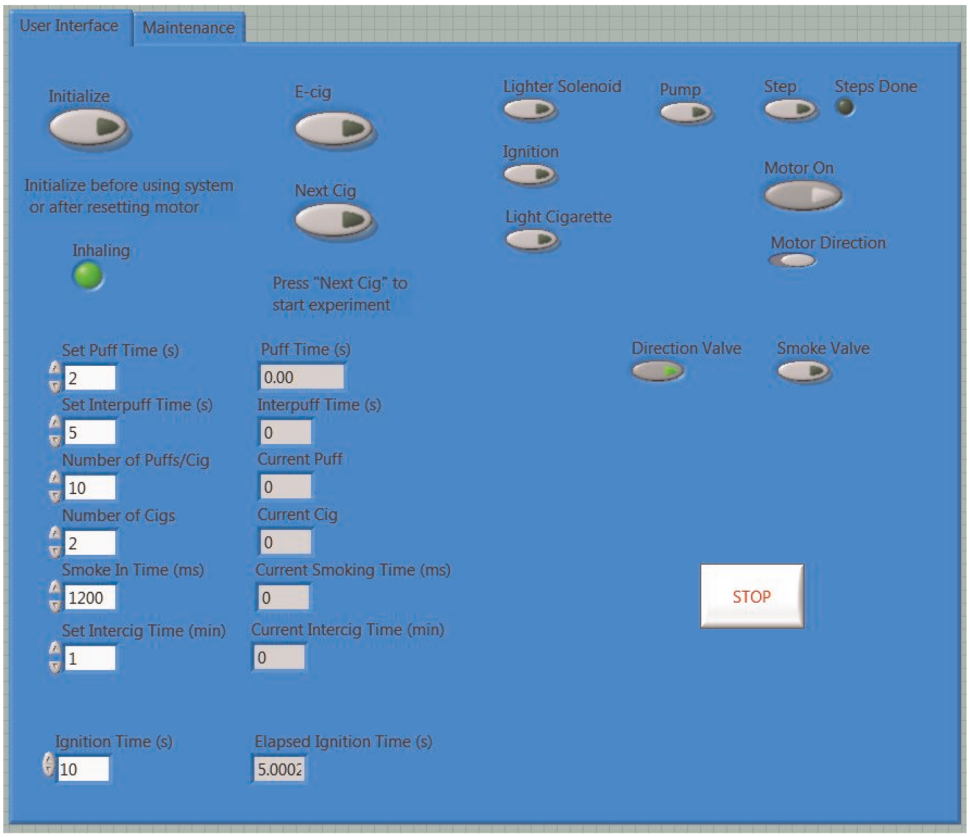
User Interface
Maintenance
Initialize
E-cig
Lighter Solenoid
Pump
Step
Steps Done
Ignition
Motor On
Initialize before using system or after resetting motor
Next Cig
Light Cigarette
Motor Direction
Inhaling
Press "Next Cig" to start experiment
Set Puff Time (s)
2
Puff Time (s)
0.00
Direction Valve
Smoke Valve
Set Interpuff Time (s)
5
Interpuff Time (s)
0
Number of Puffs/Cig
10
Current Puff
0
Number of Cigs
2
Current Cig
0
Smoke In Time (ms)
1200
Current Smoking Time (ms)
0
STOP
Set Intercig Time (min)
1
Current Intercig Time (min)
0
Ignition Time (s)
10
Elapsed Ignition Time (s)
5.0002

b

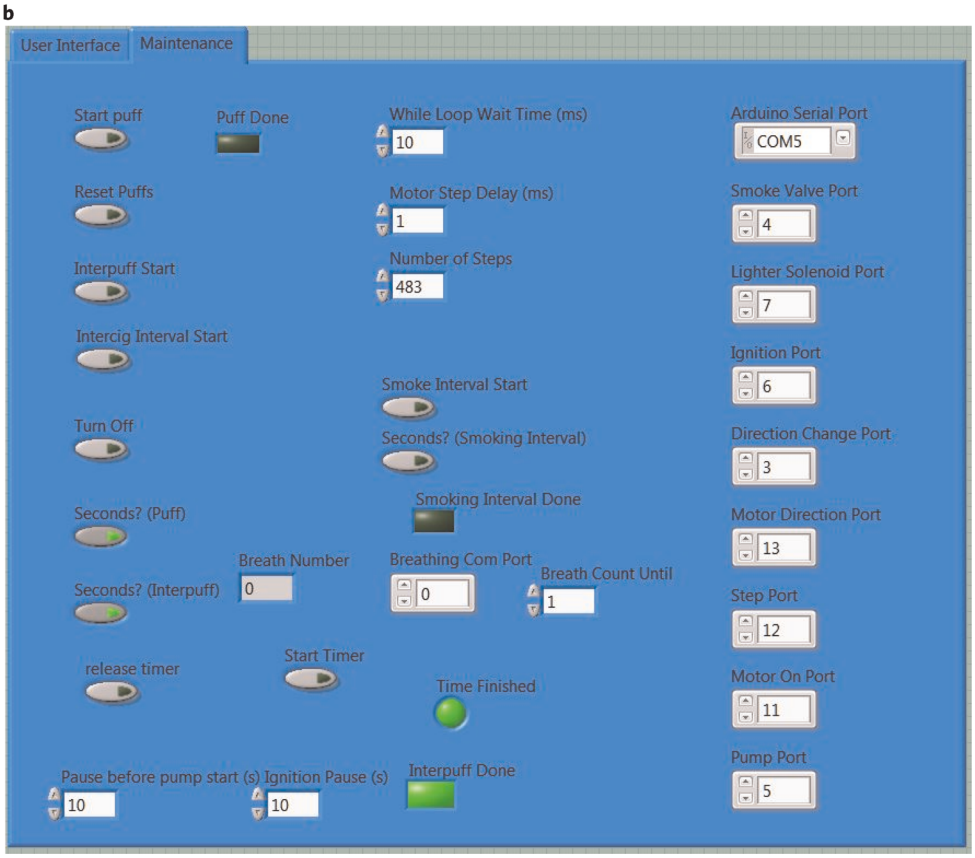
User Interface
Maintenance
Start puff
Puff Done
While Loop Wait Time (ms)
10
Arduino Serial Port
COM5
Reset Puffs
Motor Step Delay (ms)
1
Smoke Valve Port
4
Interpuff Start
Number of Steps
483
Lighter Solenoid Port
7
Intercig Interval Start
Ignition Port
6
Smoke Interval Start
Turn Off
Seconds? (Smoking Interval)
Direction Change Port
3
Smoking Interval Done
Seconds? (Puff)
Motor Direction Port
13
Breath Number
Breathing Com Port
Breath Count Until
Seconds? (Interpuff)
0
0
1
Step Port
12
release timer
Start Timer
Motor On Port
Time Finished
11
Pump Port
Pause before pump start (s)
Ignition Pause (s)
Interpuff Done
10
10
5

◀ **Fig. 5 | Software interface. a**,**b**, Screenshots of the LabVIEW user interface that is used to program and run an automated smoke exposure study (**a**) as well as set up or modify an instrument (**b**). Instrument programming can be readily performed by users with minimal instruction. Supplementary Video 1 highlights the graphical user interface regions in greater detail.

- Corning syringe filter (pore size 0.2 μm; Sigma-Aldrich, cat. no. CLS431219)
- Transwell polyester membrane inserts (6.5-mm with 0.4-μm pore; Corning, cat. no. 3470)
- RNeasy Mini Kit (Qiagen, cat. no. 74104)
- RNase-Free DNase Set (Qiagen, cat. no. 79254)
- SuperScript Reverse Transcriptase III Kit (Thermo Fisher Scientific, cat. no. 18080093)
- iTaq Universal SYBR Green Supermix (Bio-Rad, cat. no. 1725122)
- Nuclease-free water (Thermo Fisher Scientific, cat. no. AM9937)
- GeneChip Human Gene 2.0 ST Array (Affymetrix, Dana Farber Microarray Core)
- Radio-immunoprecipitation (RIPA) lysis and extraction buffer (Life Technologies, cat. no. 89900)
- Polyacrylamide (Sigma-Aldrich, cat. no. 92560) **! CAUTION** Wear safety glasses, impervious clothing, a respirator and face protection. Handle polyacrylamide with gloves. This chemical may form combustible dust concentrations in air.
- Anti-nuclear factor (erythroid-derived 2)-like 2 (Nrf2) (phospho S40) antibody (Abcam, cat. no. ab76026)
- Anti-GAPDH antibody (Millipore, cat. no. MAB374)
- Goat anti-rabbit IgG (H+L) secondary antibody (HRP-conjugated; Thermo Fisher Scientific, cat. no. 65-6120)
- Goat anti-mouse IgG (H+L) secondary antibody (HRP-conjugated; Thermo Fisher Scientific, cat. no. 62-6520)
- Horseradish peroxidase-conjugated goat anti-rabbit or mouse antibody
- Pierce ECL Plus western blotting substrate (Life Technologies, cat. no. 32132)
- MILLIPLEX MAP human cytokine/chemokine magnetic bead panels for IL-8 and MMP-1 (Millipore, cat. nos. HCYTMAG60-1xPLEX and HMMP2MAG-55K-1xPLEX)
- qPCR primers (Integrated DNA Technologies, custom order)
- SuperScript Reverse Transcriptase III (Life Technologies, cat. no. 18080-044)
- iTaq Universal SYBR Green Supermix (Bio-Rad, cat. no. 1725121)
- Sodium deoxycholate (Sigma-Aldrich, cat. no. D6750) **! CAUTION** Wear safety glasses, impervious clothing and face protection. Handle sodium deoxycholate with gloves. This chemical causes skin sensitization and eye and skin irritation.
- Sodium dodecyl sulfate (Sigma-Aldrich, cat. no. L3771) **! CAUTION** Wear safety glasses, impervious clothing and face protection. Handle sodium dodecyl sulfate with gloves. This chemical is flammable, is corrosive and causes skin sensitization and eye and skin irritation.
- Nitrocellulose membranes for western blotting (Life Technologies, cat. no. LC2009)
- Tween 20 (Sigma-Aldrich, cat. no. P9416) **! CAUTION** Wear safety glasses, impervious clothing and face protection. Handle Tween 20 with gloves.
- Ethanol
- Tris-HCl
- NaCl
- NP-40
- Formlabs Hi-Temp Resin
- Acura 60 resin
- Nonfat milk (5%)
- NiChrome wire (McMaster-Carr, cat. no. 8880K84)
- Tygon 3350 tubing
- USB cable

Equipment

- QuantStudio 7 Flex Real-Time PCR System (Life Technologies)
- Epilog 75-W laser cutter
- Peristaltic pump (Ismatec, IPC-N series)
- Organ chip holder

- Reservoir holder
- Rack holder
- Inverted transmission microscope (Zeiss, model no. AxioObserver Z1)
- High-speed camera (Hamamatsu, model no. ORCA-Flash 4.0)
- Western blotting transfer system (Bio-Rad, Criterion model)

Laser cutting
- CAD and DXF files for all parts are available in the Supplementary Data
- Smoke machine 6-mm acrylic part patterns for laser cutter (6mm.dxf, Supplementary Data)
- Smoke machine 3-mm acrylic part patterns for laser cutter (3mm.dxf, Supplementary Data)
- 3- and 6-mm-thick acrylic sheets (McMaster-Carr, cat. nos. 85635K471 and 85635K531)

Gasket fabrication
- Gasket Mold.sldprt or Gasket Mold.stl files (Supplementary Data)
- Gasket molding silicone (Quantum Silicones, cat. no. QM270)
- Die-cut polyurethane sheet (1/8-inch thick, 60 Shore A Durometer glossy black polyurethane, 2 inches × 3 inches; Atlantic Gaskets)
- Petri dish (100-mm diameter or larger) or other support for mold to avoid spillage
- Oven set to 60 °C

Smoke generator and microrespirator construction
- Microrespirator CAD files and full materials list are available in the Supplementary Data 1
- Smoke generator CAD files and full materials list are available in the Supplementary Data 2

Incubator installation
- Forma Steri-Cycle CO_2 incubator (Thermo Fisher Scientific, cat. no. 370) or similar incubator set to 37 °C and 5% CO_2
- Smoke containment enclosure and vent for incubator. A custom enclosure connected to industrial exhaust should be constructed around any incubators to be used for smoking experiments to mitigate smoke exposure to researchers. Evaluation of air flow should be performed by qualified personnel to ensure optimal performance

Computer and software
- A standard laptop or desktop running Windows 7 Intel core i5 processor, 10-GB disk space, 4 GB RAM or higher
- LabVIEW 2012 Service Pack 1 or higher (National Instruments, http://www.ni.com/download/labview-development-system-2012-sp1/3692/en/)
- Smoke Machine.vi (Supplementary Data 3)
- Timer (SubVI).vi (Supplementary Data 3)
- LINX Vis for LabVIEW (https://www.labviewmakerhub.com/doku.php?id=libraries:linx:start)
- Arduino IDE (https://www.arduino.cc/en/Main/Software)
- Affymetrix Power Tools (https://www.thermofisher.com/us/en/home/life-science/microarray-analysis/microarray-analysis-partners-programs/affymetrix-developers-network/affymetrix-power-tools.html)
- MATLAB (MathWorks, https://www.mathworks.com/products/matlab.html)
- Database for Annotation, Visualization and Integrated Discovery (DAVID) (https://david.ncifcrf.gov/tools.jsp)
- ImageJ (https://imagej.nih.gov/ij/)
- Microrespirator Software.ino (Supplementary Data 3)

Procedure

Laser cutting of acrylic sheets

1 Laser-cut acrylic sheets using a laser cutter with recommended settings for 3- and 6-mm-thick acrylic (e.g., https://www.epiloglaser.com/downloads/pdf/extt_manual.pdf). For an Epilog 75-W laser cutter, acrylic can be cut with the following settings: 3-mm acrylic: speed 20, power 75, frequency 5,000; 6-mm sheets: speed 12, power 80, frequency 5,000.
! CAUTION Fire hazard: observe laser-cutting process and clean laser cutter of debris to reduce risk of fire.

Gasket fabrication

▲ **CRITICAL** Two gaskets are needed per cigarette or e-cigarette for a total of 20 gaskets for the full BSR.

2 Obtain 3D-printed gasket molds by printing the CAD model (Supplementary Data) using in-house printing facilities or a commercial vendor. Example suitable mold materials include Formlabs Hi-Temp resin and Acura 60 resin.

3 Thoroughly mix at least 20 g of gasket molding silicone at a 10:1 ratio of component A to component B.

4 Pour the mix into a 3D-printed gasket mold placed inside a Petri dish, overfilling the cavities.

5 Place die-cut polyurethane sheet over the filled mold, starting at one edge to avoid trapping bubbles, and compress lightly.

6 Cure gaskets in oven at 60 °C overnight.

7 Remove gaskets from molds, use forceps to remove silicone flashing to achieve clear center bores, and store for smoking experiments.

■ **PAUSE POINT** Gaskets can be stored indefinitely at room temperature (18–24 °C).

Construction of the smoke generator module

▲ **CRITICAL** The Arduino should be pre-installed with LINX software as indicated in the LINX user instructions to enable communication with LabVIEW. Specific in/out connections to the Arduino can be adjusted as needed in the control software. The following steps are required to complete the assembly of the smoke generator once the permanent hardware and electronics are in place, but these steps are also required for replacement of smoke-contacting interfaces before each study.

8 Attach the smoke exhaust module to the top surface of the smoke containment module. Refer to Supplementary Fig. 2 to visualize the assemblies of both modules and their union.

9 Fasten the mouthpiece module into the SGA by threading the partially threaded rods of the mouthpiece module into the holes in the bisecting wall of the base frame module. Refer to Supplementary Fig. 3b,d to visualize the assembly and placement of the mouthpiece module.

10 Mount the motor drive and electronic components into the SGA. Refer to Supplementary Fig. 3b,c to visualize the placement and wiring configuration of components in the SGA.

11 Insert the smoke wheel module into the SGA by passing its axle through concentric openings of the bearings and tooth gears of the motor drive components. Refer to Supplementary Fig. 3a,b to visualize the assembly and placement of the smoke wheel module. The springs from the mouthpiece module should push Teflon mouthpiece through an opening in the wall holding the smoke wheel discs toward the backside of the fixed smoke wheel module, which will enable it to collect cigarette smoke from a lit cigarette held by the silicone gaskets.

12 Insert the adjustable ignition module into the SGA. The ignition module should be positioned such that the NiChrome wire touches against the tip of a cigarette when the linear actuator is fully actuated. Refer to Supplementary Figs. 4 and 5b to visualize the assembly and placement of the ignition module.

13 Cover the base frame module containing the electronics, smoke wheel and ignition modules with the assembled smoke exhaust and containment module from Step 8. The smoke containment module can be fixed onto the base frame by aligning screws and nuts from the holes of the front and back walls of the containment module through the brackets on the base frame module. The inside of the SGA can be accessed using the sliding doors from the smoke containment module. Refer to Supplementary Fig. 5 to visualize the assembly of the base frame module and the overall smoke generator. Connect smoke reservoir, air filter and tubing for air and smoke according to the diagram (Fig. 4) using Tygon 3350 and 1/4-inch-i.d. Tygon tubing as indicated. Insert tubing into the two pinch valves as indicated in Fig. 4.

▲ **CRITICAL STEP** The disposable air filter protects the pump from tar residue and resulting reduction in air flow rate and eventual pump failure.

▲ **CRITICAL STEP** The orientation of the tubing in the pinch valves is critical to achieving desired control of air and smoke flow. Be sure to insert tubing into the normally open or normally closed valve regions according to the diagram.

14 Connect 1/2-inch-i.d. Tygon tubing to the exhaust vent intake barb and cap with an air filter.

15 Construct a branched tree for the desired number of organ chips using Tygon 3350 tubing and terminate each output with a stainless-steel pin connector.

16 Connect tubing tree to the ‘smoke out’ barb on the smoke generator. The ‘smoke out’ barb is attached to the mouthpiece module (Supplementary Fig. 3d).

17 Connect a short section of Tygon 3350 tubing to the ‘air in’ barb and cap with a sterile filter.

Construction of the microrespirator module

18 Assemble the main microrespirator frame using t-slot aluminum extrusions, brackets and bolts. Refer to Supplementary Fig. 6a–d to visualize the assembly.

19 Mount the dual stepper motors with shaft couplers into the frame. Refer to Supplementary Fig. 6a to visualize the stepper motor placement.

20 Attach syringe mounts into the frame and align and fix in place eight gas-tight glass syringes. Refer to Supplementary Fig. 6b to visualize the syringe mount placement.

21 Mount piston driver mounting plate onto the 0.5-ml gas-tight syringes. Refer to Supplementary Fig. 6c to visualize the mounting plate placement.

22 Attach linear motion shafts to the piston plate and add threaded rods between the piston plate and motor couplers. Refer to Supplementary Fig. 5d to visualize the placement of linear motion shafts and threaded rods.

23 Add limit switches and fans, and tighten all components. Refer to Supplementary Fig. 6d to visualize the placement of limit switches and fans.

24 Complete wiring according to the provided wiring diagram (Supplementary Fig. 6e).

Installation into the incubator

25 Install a section of 1/2-inch-i.d. Tygon tubing, two standard power cables and a USB cable through the incubator port. The tubing should be long enough to reach from the smoke generator in the incubator to the smoke exhaust vent for the incubator enclosure that leads to an appropriate laboratory exhaust.
▲ **CRITICAL STEP** To achieve proper sealing of the incubator for stable temperature and humidity control, cut or otherwise shape the access port stopper to conform to the tubing and cables.
? TROUBLESHOOTING

26 Install peristaltic pump, organ chip holder and reservoir holder and connect power cable.

27 Mount the microrespirator in the incubator and connect the wiring to the control box magnetically attached to the outside. It is designed to slide into a rack holder or hang on the side of the incubator.

28 Install the smoke generator above the peristaltic pump and plug in the power cable and USB cable.

29 Connect the respirator status wires between the microrespirator and smoke generator to enable communication of air direction.

30 Connect 1/2-inch-i.d. Tygon tubing to the smoke generator output barb.

31 Connect the smoke generator to the computer with a USB cable and switch on the power. Venting fans will operate while the system is powered.

Software setup and parameter programming

32 Install LabVIEW 2012 on a computer and, open Smoke Machine.vi to open the user interface view (Fig. 5a).

33 In the 'Maintenance' tab (Fig. 5b), select the serial port that is connected to the Arduino.

34 Start the application to initialize communication with the BSR.

35 In the 'Maintenance' tab, select port numbers that control the components.
▲ **CRITICAL STEP** The visual switches in the 'User Interface' tab enable convenient troubleshooting and optimization of the system during initial setup and testing but should not be clicked for automated operation.

36 In the 'User Interface' tab (Fig. 5a), enter the smoking topography settings into the left column. The display boxes to the right of each parameter display the current state of the system during operation.
(Optional) For e-cigarettes or any other input sample that does not require periodic replacement, press the E-cig button to disable the rotating cigarette holder wheel.
? TROUBLESHOOTING

37 Turn on the microrespirator module and select the desired respiration volume. Start the breathing cycles using the touch screen button.
? TROUBLESHOOTING

38 Press the 'Initialize' button to initialize the hardware.

39 Press 'Next Cig' to start a test of the experiment and confirm that all steps occur as programmed.
▲ **CRITICAL STEP** This can be done with or without cigarettes. For initial setup of the BSR, full testing with cigarettes is recommended to validate ignition settings and overall stability.

Fabrication of the small airway chip

40 Follow the steps under Methods 3.1 (to fabricate the small airway chips) and 3.2–3.5 (to develop microchip clamps, chip-carrying cartridges, cartridge docks and effluent collectors, which are accessory parts for positioning and operating the small airway chips) from our previously published protocol[12].

Culture of primary lung cells in the microfluidic small airway chip

41 In a biosafety cabinet, introduce freshly prepared extracellular matrix (ECM) coating solution (e.g., rat-tail or human collagen type I, 300 μg/ml) into each of the upper and lower microfluidic channels and incubate the device overnight at 37 °C in a humidified incubator.

42 The next day, aspirate the ECM coating solution and wash the device by filling the microchannels with epithelial pre-ALI (also termed 'Submerged') medium as described in ref. [12].

43 Prepare a cell suspension of primary human small airway epithelial cells at a 2–5 × 10^6 cells/ml density.

44 Add 40 μl of the cell suspension to the upper microchannel of the chip and incubate at a 37 °C in a humidified incubator for 4–6 h.

45 Inspect the device under a microscope to ensure cell adhesion to the porous membrane throughout and then, in the biosafety cabinet, replace the culture medium in the top microchannel with fresh Submerged medium.

46 Connect the inlet port of the bottom microchannel to the medium reservoir and its outlet port to a peristaltic pump to flow medium at a 60 μl/h rate[12].

47 Replace the upper microchannel medium with fresh pre-warmed Submerged medium daily until the cells reach full confluency (~4–5 d following seeding).

48 At this point, introduce an ALI by removing medium from the upper channel and replacing the Submerged medium in the reservoir with ALI medium[12].

49 Maintain the epithelial cells under ALI for 3–5 weeks to allow full differentiation into pseudostratified mucociliated epithelium, when they will be ready for inhaled smoke/vapor exposure.

Smoke exposure of small airway organ chips

50 Place matured organ chips into the smoking incubator.

51 Connect the tubing for medium perfusion from the peristaltic pump to the basal channel of the organ chips.

52 Connect the branched tubing tree from the smoke generator to one apical channel port on the organ chips.

▲ **CRITICAL STEP** If using a conventional static in vitro exposure module[15], the smoke generator's tubing would connect to the module's gas inlet.

53 Connect the other apical channel port to the microrespirator tubing.

▲ **CRITICAL STEP** If using a conventional static in vitro exposure module[15], the exhaust outlet of the module should be connected to the microrespirator. Ensure an appropriate syringe size is selected based on the volume needed to fill up the chamber with smoke.

54 Insert cigarettes into the smoke wheel holders with gaskets.

55 Align the mounting hole before the first cigarette to be smoked with the mouthpiece. The program moves the smoke wheel one position at the start of each program.

? TROUBLESHOOTING

56 Press the 'Initialize' button to initialize the hardware. This will enable the motor.

57 Press the 'Next Cig' button to move to the next cigarette position and start the experiment. The experiment will conclude with a window stating that the set program has ended.

▲ **CRITICAL STEP** Non-smoking control chips must be located in a different tissue culture incubator and exposed (under the breathing function of the microrespirator) to humidified 37 °C air, instead of WCS, during the same time period that smoking chips received fresh WCS.

? TROUBLESHOOTING

Cleanup

58 Stop peristaltic pump perfusion with the 'stop' button.

59 Remove organ chips from the smoking incubator and place them in a second standard incubator for further culture or use in endpoint assays.

60 Close LabVIEW.

61 Turn off the microrespirator and smoke generator and unplug the USB cable.

▲ **CRITICAL STEP** Leaving the power on or the USB cable plugged in may cause exhaust fans to continue to run, resulting in excess condensation in the exhaust tubing.

62 Remove cigarette waste and tubing exposed to smoke and dispose of them in accordance with hazardous waste guidelines.

! CAUTION Residue from cigarette combustion contains carcinogens and should be handled with care.

63 Wipe interior of smoke generator with ethanol to remove accumulated residue.

64 To analyze the resultant organ chips, follow option A to perform qRT–PCR analysis, option B for whole-genome microarray expression analysis, option C for western blot analysis or option D for analysis of CBF.

(A) **Quantitative RT–PCR analysis**

(i) Isolate total RNA by lysing the cells in situ on chip and then using the RNeasy Mini Kit and following the manufacturer's protocol.

(ii) Treat the extracted RNA with DNase I for 15 min at room temperature to remove contaminating genomic DNA.

(iii) Generate cDNA using a SuperScript Reverse Transcriptase III Kit and following the manufacturer's protocol.

(iv) Perform qPCR using a real-time thermal cycler (e.g., QuantStudio 7 Flex Real-System) as previously described[2,4,34]. In brief, prepare 20-µl reactions and run conditions in triplicates. For each reaction, mix 2 µl of cDNA with 10 µl of 2 × Universal SYBR Green Supermix, 3 µl of forward primer (2 µM working concentration), 3 µl of reverse primer (2 µM working concentration) and 2 µl of molecular biology–grade water. Non-template controls should be included (in which cDNA is replaced with water).

(v) Calculate change in mRNA expression levels of target gene (e.g., heme oxygenase 1 (*HMOX1*): forward: ACTTTCAGAAGGGCCAGGTG; reverse: GACTGGGCTCTCCTTGTTGC) by normalizing against housekeeping gene (e.g., hypoxanthine-guanine phosphoribosyl transferase (*HPRT*): forward: GACTTTGCTTTCCTTGGTCAGG; reverse: AGTCTGGCTTATAT CCAACACTTCG) by $2^{-\Delta\Delta Ct}$ comparative method as previously reported[34].

(B) **Whole-genome microarray expression analysis**

(i) Isolate total RNA from smoking and non-smoking chips as discussed above (Step 64A(i)) and submit to a suitable facility for microarray analysis, using Affymetrix Human Gene ST 2.0 arrays.

(ii) Normalize the expression/intensity data by robust multi-array average and perform quality control (e.g., using Affymetrix Power Tools) as necessary.

(iii) Conduct analysis using desired programming interface. In our studies[2], we developed custom scripts in MATLAB (available upon request) and removed duplicate genes and data lacking gene IDs. Next, we compared the smoke-exposed condition against donor-matched non-exposed chips, identified genes with both a Student's *t*-test *P*-value < 0.05 and a fold-change ≥ 2 for both non-COPD and COPD donor chips to create lists of significant genes for both healthy and diseased conditions. For differential gene expression, means were subtracted and standard deviations were error-propagated. We generated heat maps using clustering linkages based on mean Euclidean distance for both biological samples and individual genes, and applied the DAVID software[35] to further break down the significant gene lists into functional processes with *P*-values < 0.05. *P*-values were corrected for multiple sampling using the Benjamini–Hochberg correction method, which decreases the false-discovery rate.

(C) **Western blot analysis**

(i) Lyse the cells in situ on-chip, using RIPA buffer (50 mM Tris-HCl, 150 mM NaCl, 1% (vol/vol) NP-40, 0.5% (wt/vol) sodium deoxycholate and 0.1% (wt/vol) sodium dodecyl sulfate).

(ii) Fractionate the proteins by SDS–PAGE.

(iii) Transfer the proteins to a nitrocellulose membrane using a commercial transfer apparatus (e.g., Bio-Rad Western Blotting Transfer System).

(iv) Block nonspecific sites in the membrane by incubating overnight in 5% nonfat milk in Tris-buffered saline–Tween 20 (TBS-T) (50 mM Tris-HCl, 150 mM NaCl, 0.1% Tween 20) at 4 °C.

(v) Incubate the membrane with primary (rabbit anti-human S40-phsophorylated Nrf2 or mouse anti-human GAPDH) antibodies overnight at 4 °C.

(vi) Perform three membrane washes in TBS-T and then incubate the membrane with secondary (horseradish peroxidase-conjugated goat anti-rabbit or mouse) antibody for 1 h at room temperature.

(vii) Develop the membrane (e.g., using the ECL Plus system) and take an image of the blot.

(D) **Analysis of CBF**

(i) Analyze the CBF by applying Fourier spectral analysis to bright-field video recordings of the ciliated surface.

(ii) For this, acquire live recordings (2–5 s each) of the ciliated surfaces at ~200 Hz (frames per s) and 512 × 512-pixel resolution using an inverted transmission microscope.
▲ **CRITICAL STEP** Because the normal range of CBF can go as high as 22 Hz, it is ideal to have a fast camera that can acquire images at ≥30 Hz. The higher the acquisition rate, the better the resolution for downstream analysis.

(iii) Capture 5–10 fields of view (FOVs) per chip, each spanning 166 × 166 μm^2.

(iv) Identify regions of ciliary motion by calculating the standard deviation of brightness at each pixel over time in each FOV in the ImageJ software (high standard deviation values correspond to notable dynamic changes in pixel brightness, which in turn indicate motion and hence ciliary beating).

(v) In the MATLAB software, threshold the areas with ciliary motion and sample randomly once per 10 μm^2 to obtain a map of CBF at single-cell resolution.

(vi) Next, determine the average CBF at each sample point from the time-dependent pixel brightness of up to 300 neighboring pixels (each pixel's signal would reflect the periodicities of the ciliary movement).

(vii) Apply a bandwidth filter of 1–30 Hz to remove noise, a Hamming window to reduce sampling artifacts, and fast Fourier transform to convert the temporal signal to the frequency domain.

(viii) Finally, for each FOV, compute the average CBF to obtain 5–10 data points per chip and compare between conditions.

(ix) For statistical analysis of CBF across different chip conditions, apply Shapiro–Wilk test (alpha level 0.05) to identify normal Gaussian distribution and non-parametric Ansari–Bradley test to study inequality of population variance (alpha level 0.05).

Troubleshooting

Troubleshooting advice can be found in Table 1.

Table 1 | Troubleshooting table

Step	Problem	Possible reason	Solution
25	Smoke does not vent properly	Exhaust tubing could be occluded by condensed water vapor from the incubator	Drain tubing regularly. Incorporation of an easily accessible drain port can simplify the process
36	Switching between cigarettes and e-cigarettes fails	E-cigarettes are much heavier than traditional cigarettes and can droop over time, losing sealing or alignment	A mechanical support or cradle can avoid this issue. Alternatively, the revolver and gaskets can be optimized for a tighter fit
		E-cigarettes are rotated out of the mouthpiece after several puffs	The 'E-cig' button should be selected for e-cigarettes to avoid motor actuation of the revolver
37	LabVIEW Software does not detect Arduino	Port not configured correctly; LINX driver not installed	Verify LINX driver has been installed; verify computer is detecting Arduino on selected port
55	Cigarettes not aligned with mouthpiece	Step count is wrong; initial alignment is incorrect; motor slips during operation	Verify that the number of steps required for one full smoke wheel revolution is equal to number of steps between cigarettes or number of cigarette holders; take care to precisely align the initial port with the mouthpiece; check motor and smoke wheel operation to make sure there is no excessive friction that could result in motor slipping
57	Cigarette is aligned but does not ignite	Ignition coil does not turn on due to poor wiring connection; ignition time not long enough; ignition coil does not contact cigarette	Test electrical continuity of the ignition coil using a multimeter; empirically determine the time required to ignite the cigarette and add 10–30% more time to account for variability; check alignment of ignition coil and adjust by realigning the ignition module or cigarette position
	Organ chips not exposed to smoke	Respirator state may be set incorrectly or not communicating; blocked tubing to microrespirator or smoke generator	Check that all tubing is free of debris and not pinched; check that the respirator state indicator light agrees with the physical motion of the microrespirator and adjust communication wire or program, if necessary

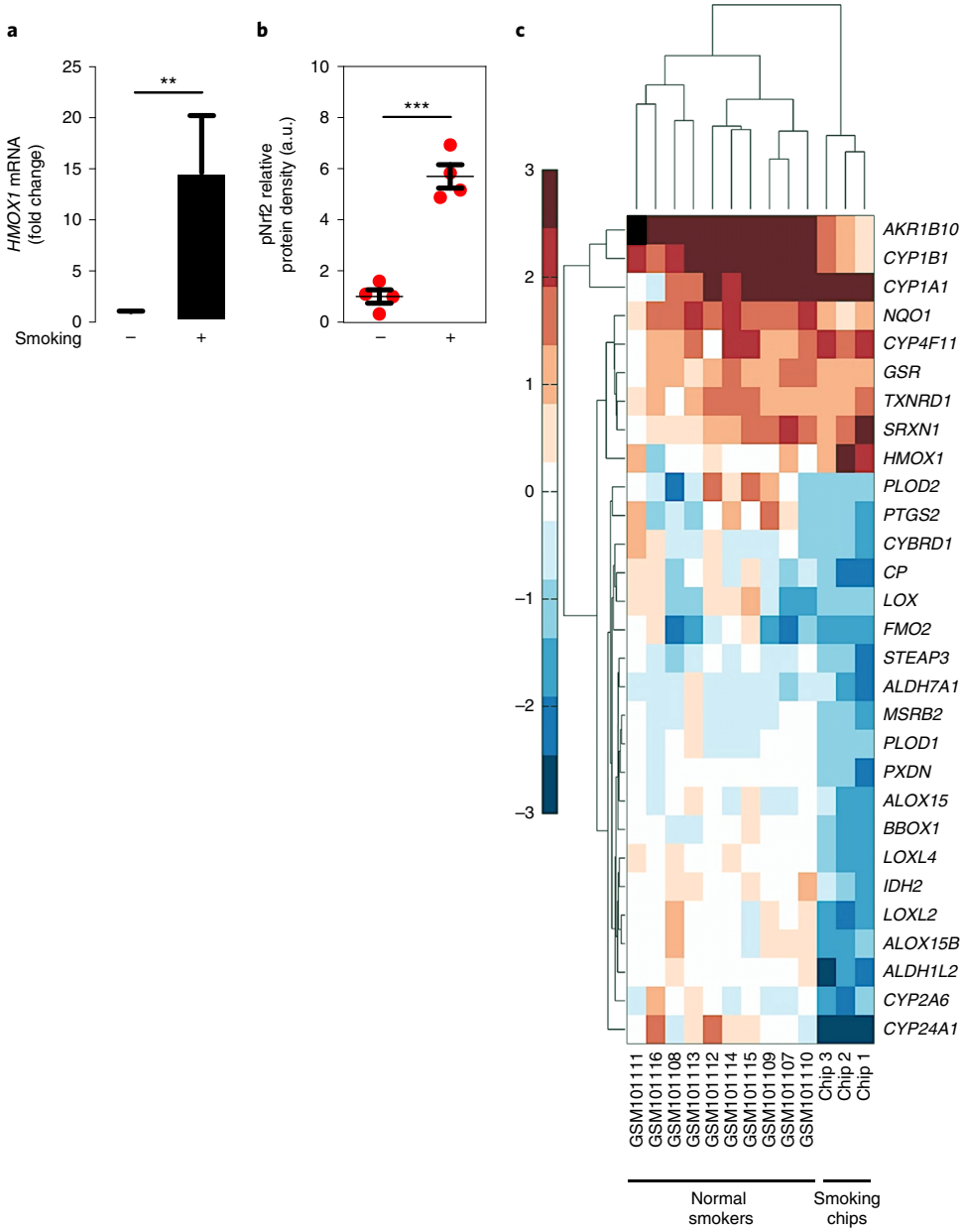

Fig. 6 | Recapitulation of smoke-induced oxidative stress by connecting microfluidic small airway chip to BSR. a,**b**, Real-time PCR and western blot analysis of induced antioxidant *HMOX1* gene expression (**$P < 0.01$; pooled data from three human donors with four biological replicate chips per donor; $n = 12$; all error bars = standard error of the mean) (**a**) and increased phosphorylation of the regulator Nrf2 (***$P < 0.001$; pooled data from two different normal human donors tested in independent experiments with two biological replicates per donor; $n = 4$) (**b**) with smoke exposure in mucociliated human bronchiolar epithelial cells on-chip. **c**, Heat map comparison of expression of 29 genes associated with cellular oxidation–reduction (identified by whole-transcriptomic analysis of smoking versus non-smoking small airway chips) against those obtained from bronchiolar epithelial cells isolated by bronchoscopy-guided brushing of small airways from ten different normal human smokers in an independent clinical study. Note the high level of similarity in expression of upregulated (red) and downregulated (blue) genes. The color map indicates log2 fold changes in gene expression. Image adapted with permission from ref. [2], Elsevier.

Timing

Step 1, laser cutting of acrylic sheets
Steps 2–7, gasket fabrication: 1 h to cast parts plus overnight curing
Steps 8–17, construction of the smoke generator module
Steps 18–24, microrespirator assembly: ~1 d
Steps 25–31, installation into incubator: 1–3 h

Steps 32–39, software programming and parameter setup: 1–2 h
Step 40, organ chip fabrication: ~ 2 d
Steps 41–49, small airway chip culture: ~3–4 weeks
Steps 50–57, smoke exposure of organ chips: 2–3 h prep time plus experiment duration
Steps 58–63, cleanup: 1 h
Step 64A, quantitative RT–PCR analysis: 3–4 h
Step 64B, whole-genome microarray expression analysis: 1–3 weeks
Step 64C, Western blot analysis: 3–6 h
Step 64D, analysis of CBF: 1–3 weeks post-acquisition

Anticipated results

This protocol provides a step-by-step procedure for engineering a microfluidically linked, modular and programmable BSR system that can be used to expose living cells within organ chips or potentially other culture systems to freshly generated whole smoke under physiological breathing airflow. The three major electromechanical components for successful setup and operation of this BSR system are (i) a smoking machine, (ii) a chip microrespirator and (iii) a synchronized programming interface. Upon manufacturing this platform, one should be able to connect it to microfluidic human lung small airway chips that have described previously[2,4] to explore biological responses of living human airway tissue isolated from any desired patient population to inhaled electronic or conventional cigarette smoke in vitro.

As a specific example, we used this instrument to sequentially create fresh WCS from nine research-grade 3R4F cigarettes over a period of 75 min, and exposed terminally differentiated human mucociliated bronchiolar epithelium in our small airway chips to the smoke under physiological breathing conditions (Fig. 1a). The next day, we analyzed the biological responses and observed more than a tenfold increase in expression of the antioxidant gene, *HMOX1*, as compared to that of untreated controls when analyzed by qPCR (Fig. 6a). In addition, there was a parallel increase in phosphorylation of the oxidation-induced cytoprotective transcription factor protein Nrf2 (Fig. 6b;

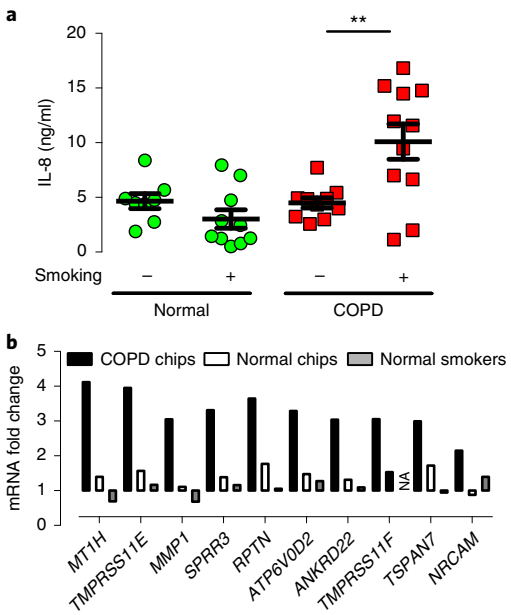

Fig. 7 | Recreating COPD exacerbation and disease-specific responses using the BSR. a, WCS exposure leads to clinically relevant selective IL-8 secretion from COPD airway epithelia on-chip (**$P < 0.01$; pooled data from five human donors, with two to five biological replicates per donor; $n = 11$). **b**, Relative expression levels of ten genes that were most significantly upregulated in COPD chips (black bars) and not upregulated in normal (healthy non-diseased) chips (white bars) after smoke exposure. Gray bars illustrate expression levels of the same genes in bronchoscopy samples of small airway epithelial cells from healthy human smokers versus non-smokers. This graph supports the biological relevance of the system (e.g., upregulation of matrix metallopeptidase 1 (*MMP1*) in COPD chips is consistent with clinical reports and the role of *MMP1* in COPD pathogenesis) and enables discovery of disease-specific responses. NA, no transcriptomic clinical data available. Image adapted with permission from ref. [2], Elsevier.

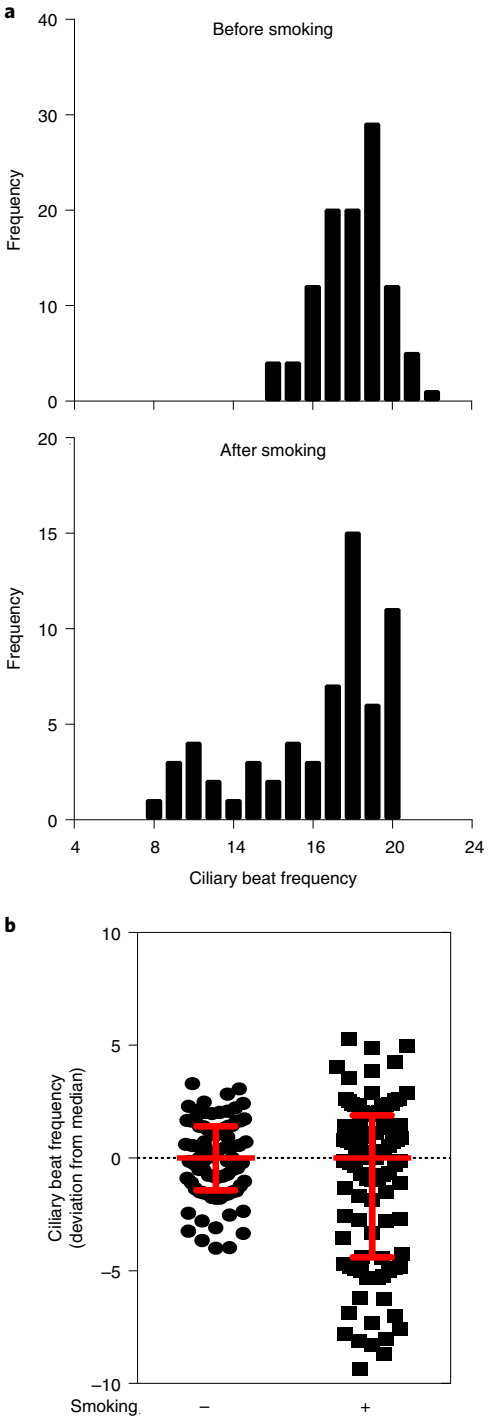

Fig. 8 | Utilization of the breathing-smoking human lung chip to characterize cigarette smoke-induced ciliary micropathologies. a, Distribution patterns of CBF in a representative normal small airway chip before and after smoking. As illustrated, the normal Gaussian distribution changes to a flattened, non-normal distribution following smoke exposure (statistically significant). **b**, Deviations from the median of CBF measurements in normal bronchiolar epithelium with (+) or without (−) exposure to WCS on-chip, 24 h after challenge (data pooled from two different human donors, with each symbol representing a measurement in 1 FOV and >70 FOVs being analyzed for each condition; control tissue exhibited a Gaussian distribution of CBFs, whereas smoke-exposed tissue did not (non-smoking: FOV $n = 80$, chip $n = 9$, Shapiro–Wilk test, $P = 0.1428$; smoking: FOV $n = 99$; chip $n = 9$, Shapiro–Wilk test; $P = 0.0002$). Note the significant variability in beating frequency due to acute smoke exposure (75 min, 9 × cigarettes). Image adapted with permission from ref. [2], Elsevier.

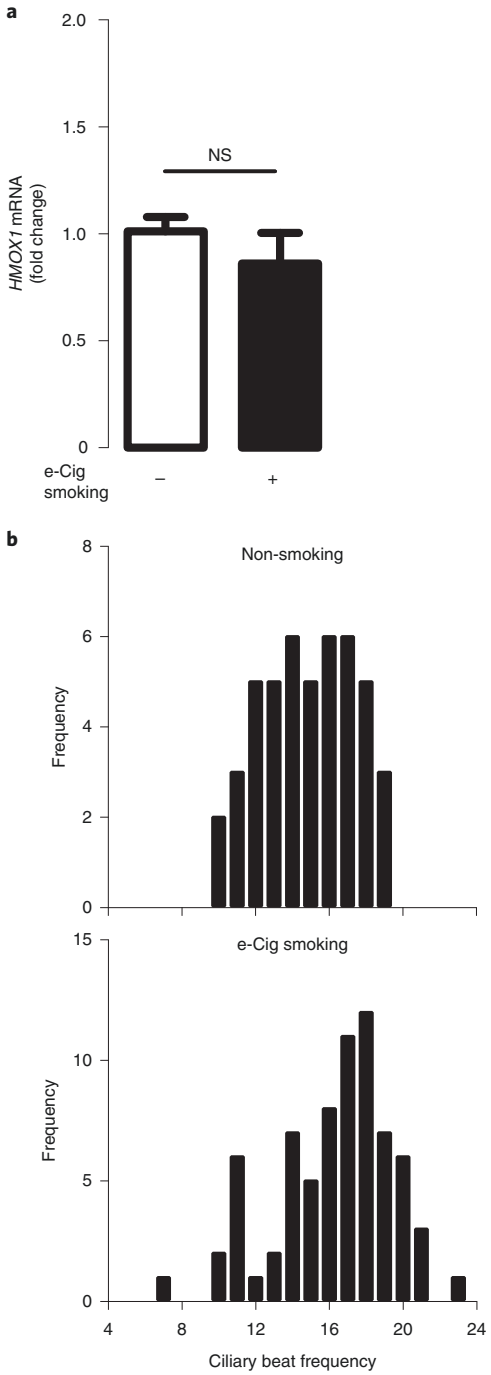

Fig. 9 | Application of the BSR to study the biological impact of e-cigarettes in vitro. a, Acute intense exposure to e-cigarette vapor (24 h after 75-min e-smoking session) did not induce expression of the antioxidant gene *HMOX1*, as quantified by qPCR (pooled data from two human donors with three to four biological replicates per donor; $n = 8$). **b**, Distribution pattern of CBF in a representative normal small airway chip exposed to e-cigarette smoke (e-smoking; bottom) against that observed in a non-smoking chip (top). Note gradual transformation of CBF from a normal bell-shaped to a bimodal distribution (in this case within the tested exposure regimen it did not reach statistical significance). Image adapted with permission from ref. [2], Elsevier.

ref. [2]). Importantly, to more comprehensively validate this model against human patient data, we performed genome-wide gene microarray analysis and compared our acute exposure results against those obtained by similar analysis of small airway epithelial cells isolated during bronchoscopy from phenotypically normal human smokers versus non-smokers, using a published dataset[36]. We found similarities between human smokers and our smoking chips for a majority of differentially expressed

genes associated with the oxidation–reduction pathway (Fig. 6c)[2]. The accession number for the transcriptomic data reported in this paper is GEO: GSE87098.

Beyond clinical validation, the value of the BSR linked to the microfluidic human small airway chip lies in three major applications: (i) recreating patient-specific responses to identify potential therapeutic targets and diagnostic/prognostic biomarkers; (ii) discovering new smoke-induced pathologies; and (iii) exploring toxicity of emerging tobacco-related products, such as e-cigarettes. Past clinical studies have revealed increased pulmonary neutrophilic accumulation and interleukin 8 (IL-8) levels in lungs of COPD patients who smoke versus lungs of healthy patients[37,38]. When we stimulated small airway chips with WCS, we observed that chips created with epithelial cells isolated from COPD patients responded by producing large increases in secretion of IL-8, whereas there was no significant change in chips lined with epithelium obtained from healthy individuals (Fig. 7a). Applying a matched comparison that corrects for inter-individual variabilities and enables biosignature discovery, we were able to use this platform to identify smoke-triggered COPD-specific gene expression responses by transcriptomic analysis (Fig. 7b). Some of these changes, such as upregulation of matrix metallopeptidase 1 (*MMP1*) in COPD chips, validated this model, as this response is in line with published clinical reports on involvement of *MMP1* in COPD pathogenesis[39,40]. Expression patterns of other genes, such as transmembrane protease serine 11E and 11F (*TMPRSS11E* and *TMPRSS11F*), small proline-rich protein 3 (*SPRR3*) and repetin (*RPTN*) revealed their induction in smoke-exposed COPD microdevices, as these genes have not been previously associated with COPD; this approach could facilitate identification of new clinical biomarkers and potential therapeutic targets.

By conducting an automated analysis of CBF in smoke-challenged versus non-exposed small airway chips, using high-speed video-microscopy, we observed that smoking transforms the normal Gaussian distribution in matched untreated samples of the same donor into a bimodal distribution, and significantly changes the variance of the ciliary beat pattern[2] (Fig. 8). The skewed CBF distributions seen in smoke-exposed samples invalidate the use of statistics and associated tests of significance that assume a normal distribution, such as the mean (average) value and the popular Student's *t*-test. In fact, this experiment helped explain conflicting reports in past studies that measured only change in average CBF following smoke exposure[41–43], by revealing true pathological endpoints for analysis.

In addition, the BSR enables investigation into the toxicity of e-cigarettes. When we exposed the human small airway chips acutely to emissions from a commercially available e-cigarette (blu) under the same exposure regimen as the 3R4F tobacco cigarettes, there was no significant change in gene expression of *HMOX-1* (Fig. 9a); however, the e-cigarette challenge changed the ciliary beating distribution from a normal Gaussian distribution to a non-normal pattern (Fig. 9b). The CBF transformation in this study (acute exposure) did not reach statistical significance but revealed a unique potential of the chip-based smoking platform for discovery of subtle phenotypic responses to emerging tobacco products without disturbing the ALI.

It is important to mention that appropriate optimization and quality control steps should be followed by the end user. For our studies, for instance, we explored whether continuous smoke exposure (by excluding inter-puff intervals) could impact cell viability. We found that this can lead to cytotoxicity (Supplementary Fig. 7a), indicating that such a pattern of smoke exposure may not be ideal when investigating the impact of WCS in the absence of cell death. Similarly, to ensure that breathing airflow per se is not a confounding factor in pathologies induced by cigarette smoke, we carried out appropriate studies and found that disease-specific upregulation of *MMP1* in COPD chips is not due to airflow shear; rather, it is triggered by smoke exposure in COPD microdevices (Supplementary Fig. 7b).

References

1. Powell, H. A., Iyen-Omofoman, B., Baldwin, D. R., Hubbard, R. B. & Tata, L. J. Chronic obstructive pulmonary disease and risk of lung cancer: the importance of smoking and timing of diagnosis. *J. Thorac. Oncol.* **8**, e34 (2013).
2. Benam, K. H. et al. Matched-comparative modeling of normal and diseased human airway responses using a microengineered breathing lung chip. *Cell Syst.* **3**, 456–466.e454 (2016).
3. Bhatia, S. N. & Ingber, D. E. Microfluidic organs-on-chips. *Nat. Biotechnol.* **32**, 760–772 (2014).
4. Benam, K. H. et al. Small airway-on-a-chip enables analysis of human lung inflammation and drug responses in vitro. *Nat. Methods* **13**, 151–157 (2016).

5. Benam, K. H. & Ingber, D. E. Commendation for exposing key advantage of organ chip approach. *Cell Syst.* **3**, 411 (2016).
6. Benam, K. H., Konigshoff, M. & Eickelberg, O. Breaking the in vitro barrier in respiratory medicine. engineered microphysiological systems for chronic obstructive pulmonary disease and beyond. *Am. J. Respir. Crit. Care Med.* **197**, 869–875 (2018).
7. Niemeyer, B. F., Zhao, P., Tuder, R. M. & Benam, K. H. Advanced microengineered lung models for translational drug discovery. *SLAS Discov* **23**, 777–789 (2018).
8. Benam, K. H. Disrupting experimental strategies for inhalation toxicology: the emergence of microengineered breathing-smoking human lung-on-a-chip. *Appl. In Vitro Toxicol.* **4**, 107–114 (2018).
9. Benam, K. H. et al. Exploring new technologies in biomedical research. *Drug Discov. Today* **24**, 1242–1247 (2019).
10. Novak, R. et al. Scalable fabrication of stretchable, dual channel, microfluidic organ chips. *J. Vis. Exp.* **140**, e58151 (2018).
11. Huh, D. et al. Microfabrication of human organs-on-chips. *Nat. Protoc.* **8**, 2135–2157 (2013).
12. Benam, K. H. et al. Human lung small airway-on-a-chip protocol. *Methods Mol. Biol.* **1612**, 345–365 (2017).
13. Gotts, J. E. et al. Cigarette smoke exposure worsens endotoxin-induced lung injury and pulmonary edema in mice. *Nicotine Tob. Res.* **19**, 1033–1039 (2017).
14. Sundar, I. K., Nevid, M. Z., Friedman, A. E. & Rahman, I. Cigarette smoke induces distinct histone modifications in lung cells: implications for the pathogenesis of COPD and lung cancer. *J. Proteome Res.* **13**, 982–996 (2014).
15. Thorne, D. & Adamson, J. A review of in vitro cigarette smoke exposure systems. *Exp. Toxicol. Pathol.* **65**, 1183–1193 (2013).
16. Thorne, D. et al. The mutagenic assessment of mainstream cigarette smoke using the Ames assay: a multi-strain approach. *Mutat. Res. Genet. Toxicol. Environ. Mutagen.* **782**, 9–17 (2015).
17. Thorne, D. et al. Characterisation of a Vitrocell(R) VC 10 in vitro smoke exposure system using dose tools and biological analysis. *Chem. Cent. J.* **7**, 146 (2013).
18. Thorne, D., Larard, S., Baxter, A., Meredith, C. & Gaa, M. The comparative in vitro assessment of e-cigarette and cigarette smoke aerosols using the gammaH2AX assay and applied dose measurements. *Toxicol. Lett.* **265**, 170–178 (2017).
19. Mathis, C. et al. Human bronchial epithelial cells exposed in vitro to cigarette smoke at the air–liquid interface resemble bronchial epithelium from human smokers. *Am. J. Physiol. Lung Cell. Mol. Physiol.* **304**, L489–L503 (2013).
20. Phillips, J., Kluss, B., Richter, A. & Massey, E. Exposure of bronchial epithelial cells to whole cigarette smoke: assessment of cellular responses. *Altern. Lab. Anim.* **33**, 239–248 (2005).
21. Scian, M. J., Oldham, M. J., Kane, D. B., Edmiston, J. S. & McKinney, W. J. Characterization of a whole smoke in vitro exposure system (Burghart Mimic Smoker-01). *Inhal. Toxicol.* **21**, 234–243 (2009).
22. Glader, P. et al. Cigarette smoke extract modulates respiratory defence mechanisms through effects on T-cells and airway epithelial cells. *Respir. Med.* **100**, 818–827 (2006).
23. Mio, T. et al. Cigarette smoke induces interleukin-8 release from human bronchial epithelial cells. *Am. J. Respir. Crit. Care Med.* **155**, 1770–1776 (1997).
24. Hellermann, G. R., Nagy, S. B., Kong, X., Lockey, R. F. & Mohapatra, S. S. Mechanism of cigarette smoke condensate-induced acute inflammatory response in human bronchial epithelial cells. *Respir. Res.* **3**, 22 (2002).
25. Anto, R. J., Mukhopadhyay, A., Shishodia, S., Gairola, C. G. & Aggarwal, B. B. Cigarette smoke condensate activates nuclear transcription factor-kappaB through phosphorylation and degradation of IkappaB(alpha): correlation with induction of cyclooxygenase-2. *Carcinogenesis* **23**, 1511–1518 (2002).
26. Carnevali, S. et al. Cigarette smoke extract induces oxidative stress and apoptosis in human lung fibroblasts. *Am. J. Physiol. Lung Cell. Mol. Physiol.* **284**, L955–L963 (2003).
27. Ween, M. P., Whittall, J. J., Hamon, R., Reynolds, P. N. & Hodge, S. J. Phagocytosis and Inflammation: exploring the effects of the components of E-cigarette vapor on macrophages. *Physiol. Rep.* **5**, e13370 (2017).
28. Hoyt, J. C. et al. Cigarette smoke decreases inducible nitric oxide synthase in lung epithelial cells. *Exp. Lung Res.* **29**, 17–28 (2003).
29. Adamson, J., Haswell, L. E., Phillips, G., & Gaça, M. D. In vitro models of chronic obstructive pulmonary disease (COPD). In *Bronchitis* (ed. Martín-Loeches, I.) (InTechOpen, 2011).
30. Rao, P., Ande, A., Sinha, N., Kumar, A. & Kumar, S. Effects of cigarette smoke condensate on oxidative stress, apoptotic cell death, and HIV replication in human monocytic cells. *PLoS ONE* 11, (e0155791 (2016).
31. Strasser, A. A. et al. Nicotine metabolite ratio predicts smoking topography and carcinogen biomarker level. *Cancer Epidemiol. Biomarkers Prev.* **20**, 234–238 (2011).
32. Hammond, D., Fong, G. T., Cummings, K. M. & Hyland, A. Smoking topography, brand switching, and nicotine delivery: results from an in vivo study. *Cancer Epidemiol. Biomarkers Prev.* **14**, 1370–1375 (2005).
33. Manigrasso, M., Buonanno, G., Fuoco, F. C., Stabile, L. & Avino, P. Aerosol deposition doses in the human respiratory tree of electronic cigarette smokers. *Environ. Pollut.* **196**, 257–267 (2015).
34. Benam, K. H., Kok, W. L., McMichael, A. J. & Ho, L. P. Alternative spliced CD1d transcripts in human bronchial epithelial cells. *PLoS ONE* **6**, e22726 (2011).
35. Huang da, W., Sherman, B. T. & Lempicki, R. A. Systematic and integrative analysis of large gene lists using DAVID bioinformatics resources. *Nat. Protoc.* **4**, 44–57 (2009).

36. Harvey, B. G. et al. Modification of gene expression of the small airway epithelium in response to cigarette smoking. *J. Mol. Med.* **85**, 39–53 (2007).
37. Keatings, V. M., Collins, P. D., Scott, D. M. & Barnes, P. J. Differences in interleukin-8 and tumor necrosis factor-alpha in induced sputum from patients with chronic obstructive pulmonary disease or asthma. *Am. J. Respir. Crit. Care Med.* **153**, 530–534 (1996).
38. Dickens, J. A. et al. COPD association and repeatability of blood biomarkers in the ECLIPSE cohort. *Respir. Res.* **12**, 146 (2011).
39. Imai, K. et al. Human collagenase (matrix metalloproteinase-1) expression in the lungs of patients with emphysema. *Am. J. Respir. Crit. Care Med.* **163**, 786–791 (2001).
40. Mercer, B. A., Kolesnikova, N., Sonett, J. & D'Armiento, J. Extracellular regulated kinase/mitogen activated protein kinase is up-regulated in pulmonary emphysema and mediates matrix metalloproteinase-1 induction by cigarette smoke. *J. Biol. Chem.* **279**, 17690–17696 (2004).
41. Stanley, P. J., Wilson, R., Greenstone, M. A., MacWilliam, L. & Cole, P. J. Effect of cigarette smoking on nasal mucociliary clearance and ciliary beat frequency. *Thorax* **41**, 519–523 (1986).
42. Yaghi, A., Zaman, A., Cox, G. & Dolovich, M. B. Ciliary beating is depressed in nasal cilia from chronic obstructive pulmonary disease subjects. *Respir. Med.* **106**, 1139–1147 (2012).
43. Zhou, H. et al. Increased nasal epithelial ciliary beat frequency associated with lifestyle tobacco smoke exposure. *Inhal. Toxicol.* **21**, 875–881 (2009).

Acknowledgements

This research was sponsored by the Wyss Institute for Biologically Inspired Engineering at Harvard University and the Defense Advanced Research Projects Agency under Cooperative Agreement no. W911NF-12-2-0036. The views and conclusions contained in this document are those of the authors and should not be interpreted as representing the official policies, either expressed or implied, of the Defense Advanced Research Projects Agency or the U.S. Government.

Author contributions

K.H.B. and R.N. led system and protocol development and conducted smoking studies; R.N. and Y.C. designed the smoking robot and control software; T.C.F. and R.N. designed the microrespirator; K.H.B., R.N. and D.E.I. wrote the manuscript.

Competing interests

D.E.I. is a founder and holds equity in Emulate, Inc. and chairs its scientific advisory board. K.H.B., R.N., Y.C. and D.E.I. are also inventors on intellectual property licensed to Emulate, Inc.

Additional information

Supplementary information is available for this paper at https://doi.org/10.1038/s41596-019-0230-y.

Correspondence and requests for materials should be addressed to D.E.I.

Peer review information *Nature Protocols* thanks Amy Ryan (Firth) and other anonymous reviewer(s) for their contribution to the peer review of this work.

Reprints and permissions information is available at www.nature.com/reprints.

Publisher's note Springer Nature remains neutral with regard to jurisdictional claims in published maps and institutional affiliations.

Received: 1 February 2018; Accepted: 24 July 2019;
Published online: 10 January 2020

Related links
Key reference using this protocol
Benam, K. H. et al. *Cell Syst.* **3**, 456-466.e4 (2016): https://doi.org/10.1016/j.cels.2016.10.003